The Danger of High-Frequency Spurious Effects on Wide Microstrip Line

Francisco Mesa, *Member, IEEE,* and David R. Jackson, *Fellow, IEEE*

***Abstract*—It has been found that remarkably severe spurious effects can occur in the current excited on microstrip line at moderate to high frequency, when the strip is wide (approximately $w/h > 3$). This newly observed effect occurs because one or more leaky modes (LMs) approaches the branch point at k_0 in the complex longitudinal wavenumber plane. When this happens, the attenuation (leakage) constant of these LMs becomes very small. Hence, the LMs can propagate to very large distances along the line with only minimal attenuation. This effect only occurs when the strip is fairly wide, and at certain frequencies. When it occurs, the effect can be disastrous since the continuous-spectrum (radiation) part of the current on the strip then decays very slowly with distance from the source so that the total strip current excited by the source exhibits spurious oscillations out to very large distances from the source. An approximate design rule for predicting this effect is given, which is accurate for wide strips (approximately $w/h > 6$). The LMs that are responsible for this effect are identified, and the behavior of these modes are studied for different strip widths.**

***Index Terms*—Leaky waves, microstrip, microwave integrated circuits, planar transmission lines, planar waveguides, printed circuits.**

I. Introduction

LEAKY MODES have been found to exist on a variety of printed-circuit transmission lines over the last couple of decades, and their properties have been extensively studied [1]–[25]. In particular, the microstrip line is one commonly used transmission-line structure for which leaky modes (LM) have been found to exist. It has been shown recently that LMs may exist on a microstrip line with an isotropic substrate, at high frequency [1]. Substrate anisotropy may also induce the existence of LMs [2]. These LMs, if excited sufficiently by a practical source, will result in significant spurious effects such as power loss and crosstalk, as well as interference with the desired bound mode (BM) that is also excited from the source. When examining the current on the strip that is excited from a practical source, this interference typically takes the form of oscillations in the total current (TC) on the strip, when plotted versus distance from the source [3]. The interference arises because the bound and LMs have different propagation wavenumbers. Usually, the interference effect dies out with distance relatively quickly (within a few wavelengths from the source) because the LM has a complex wavenumber and, hence, decays exponentially with distance from the source. Therefore, in most cases that have been previously studied, where the strip width is moderate, the excited LMs are not very important more than a few wavelengths from the source. It has been found that the spurious oscillations that are observed in the current generally increase with frequency and become significant when the substrate thickness is about one-tenth of a free-space wavelength. However, most of the spurious effects are confined to a region that is about ten wavelengths from the source [3].

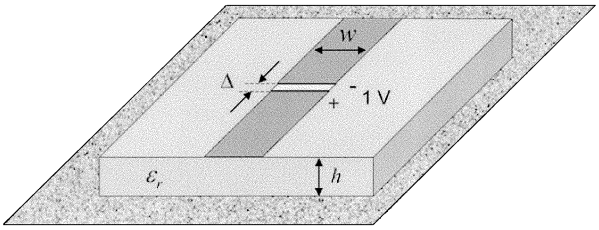

Fig. 1. Geometry of an infinite microstrip line with a 1-V gap source at $z = 0$.

In contrast, it has been discovered that when the strip is fairly *wide* $(w/h > 3)$, *important exceptions* can occur. In particular, for such wide strips, a frequency region will exist where the spurious oscillations extend out to *extreme distances* from the source, possibly as large as many tens of wavelengths. This new effect does not, in general, increase with frequency, but instead, it occurs mainly in the vicinity of certain specific frequencies, depending on the strip width. The purpose of this paper is to report this new finding and to investigate it in some detail by using a semianalytical model for the current excited on a microstrip line by a voltage gap source, as was used in [3] (and originally introduced in [4]). The geometry of the microstrip line with a voltage gap source is shown in Fig. 1.

In [3], the current excited on a microstrip line by a voltage gap source was studied for moderate strip widths. It was demonstrated that spurious oscillatory effects in the current is due to an interference between the BM of propagation (the desired mode that is normally used for signal transmission) and the *continuous-spectrum* (CS) part of the current [3], [5]. The CS (or radiating) part of the current generally increases with frequency, eventually becoming comparable in magnitude to the BM current roughly in the frequency range where the substrate thickness is about one-tenth of a free-space wavelength. However, it is not always a LM that is responsible for the increase in the CS as the frequency increases. Mathematically, the CS current on the line consists of a sum of any physical LM currents, together

Manuscript received April 3, 2002; revised August 20, 2002. This work was supported in part by the State of Texas under the Advanced Research and Technology Program. The work of F. Mesa was supported in part by the Spanish Ministry of Science and Technology and by FEDER Funds under Project TIC2001-3163.

F. Mesa is with the Department of Applied Physics I, University of Seville, Seville 41012, Spain.

D. R. Jackson is with the Department of Electrical and Computer Engineering, University of Houston, Houston, TX 77204-4005 USA.

Digital Object Identifier 10.1109/TMTT.2002.805133

with *residual-wave* (RW) currents [6]. The RW currents account for that part of the CS current that is not channeled into one or more LMs. High-frequency spurious effects on a microstrip line with a moderate strip width may be due to either a LM or a RW current (or a combination of the two [3], depending on the frequency range, the substrate permittivity, and the distance from the source). The RW currents decay algebraically with distance from the source, as opposed to the LMs that decay exponentially. Therefore, for distances that are more than a few wavelengths from the source, the high-frequency spurious effects that are observed on microstrip line with a moderate strip width are due to the RW currents. Within a few wavelengths from the source, a LM may be mainly responsible for the spurious effects, depending on the parameters [3]. In all cases, however, the trend is that the CS current continuously increases in magnitude as the frequency increases. Hence, the spurious effects continuously increase with frequency for microstrip with a moderate strip width. To avoid such effects, the frequency should be chosen low enough so that the substrate thickness is less than approximately 0.1 λ_0.

In contrast, the newly discovered effect reported here for *wide* microstrip lines occurs in a particular frequency range, which depends mainly on the width of the strip. As the width of the strip increases, the frequency at which this new effect is observed decreases. For moderately wide strips, the effects occurs only at high frequency, but for very wide strips, it may occur at moderate frequencies. The frequency range over which the effect is observed may be fairly narrow. However, when this effect does occur, the resulting interference observed in the strip current is extremely severe out to very large distance, much larger than for the moderate strip-width cases. This new effect is due to one or more LMs approaching the k_0 branch point in the longitudinal k_z wavenumber plane, which is the plane used in the construction of the current from the voltage gap source. Near the branch point, the attenuation constant of the LMs are found to be quite small so that they can propagate to very large distances before decaying significantly. This explains the long-range spurious effects that are observed. Interestingly, such effects are only observed for wide strips. When the strip width is small or moderate $(w/h < 3)$, it appears that the LMs do not typically approach the branch point. As will be demonstrated, an approximate design rule for predicting the frequency at which the LMs approach the branch point can be given. Results will be presented for various strip widths, including a moderate strip width and two large strip widths, in order to demonstrate when the effect occurs and to study the LMs that are responsible.

II. Analysis

The microstrip line is assumed to be infinitely long in the $\pm z$-directions, infinitesimally thin, and perfectly conducting. The line is excited at $z = 0$ by a 1-V gap voltage source, as shown in Fig. 1. The gap source is assumed to have a uniform impressed electric field $E_z^{\rm gap}(z)$ that exists over the region $-\Delta/2 < z < \Delta/2$. Theoretically, Δ may be chosen to be zero to represent a delta-gap source, although numerically it is chosen as $\Delta = 0.05\lambda_0$ since this makes the Fourier transform converge faster and, thus, helps with the numerical convergence. (For distances more than a fraction of a wavelength from the source, the value of Δ is inconsequential.) The current density on the strip is represented in a basis function expansion as

$$J_{sz}(x,z) = \sum_{m=0,2\ldots} T_m^z(x) I_m^z(z) \tag{1a}$$

$$J_{sx}(x,z) = \sum_{n=1,3\ldots} T_n^x(x) I_n^x(z) \tag{1b}$$

where the transverse shape functions $T_m^z(x)$ and $T_n^x(x)$ are chosen to be Chebyshev polynomials weighted by appropriate edge-singularity terms [7]. In particular,

$$\begin{aligned} T_m^z(x) =& \frac{2}{w\delta_m} \frac{T_m\left(\frac{2x}{w}\right)}{\sqrt{1-\left(\frac{2x}{w}\right)^2}} \\ T_n^x(x) =& j\frac{4}{w\pi} U_n\left(\frac{2x}{w}\right)\sqrt{1-\left(\frac{2x}{w}\right)^2} \\ \delta_m =& \begin{cases} \pi, & m=0 \\ \dfrac{\pi}{2}, & m>0 \end{cases} \end{aligned} \tag{2}$$

where T_m and U_n are the Chebyshev polynomials of the first and second kind, respectively.

A multiple basis function expansion is needed for accurate results since wide strips will be investigated. The total longitudinal current on the strip is described by the function $I_0^z(z)$ since the integral across the strip width of $T_m^z(x)$ is unity for $m = 0$ and zero for $m > 0$. The electric-field integral equation (EFIE) is used, which equates the tangential electric field on the strip to that of the impressed gap voltage at the source, and zero on the metal strip. The EFIE is written in the spectral domain using the spectral-domain Green's function for the layered structure. The Fourier transform of the EFIE with respect to z is taken, and then the functions $T_m^z(x)$ and $T_n^x(x)$ are used as testing functions. This results in a matrix equation of the form

$$\begin{bmatrix} [\Gamma_{mp}^{zz}(k_z)] & [\Gamma_{mq}^{zx}(k_z)] \\ [\Gamma_{np}^{xz}(k_z)] & [\Gamma_{nq}^{xx}(k_z)] \end{bmatrix} \cdot \begin{bmatrix} \left[\tilde{I}_p^z(k_z)\right] \\ \left[\tilde{I}_q^x(k_z)\right] \end{bmatrix} = \begin{bmatrix} [b_m(k_z)] \\ [0] \end{bmatrix} \tag{3}$$

where

$$b_m(k_z) = \tilde{E}_z^{\rm gap}(k_z) \int_{-w/2}^{w/2} \left[T_m^z(x)\right] dx. \tag{4}$$

and

$$\Gamma_{ij}^{\alpha\beta}(k_z) = \frac{1}{2\pi} \int_{C_i} \tilde{T}_i^{\alpha}(-k_x) \tilde{G}_{\alpha\beta}(k_x,k_z) \tilde{T}_j^{\beta}(k_x) dk_x \tag{5}$$

where C_x is a path from $-\infty$ to ∞ in the complex k_x (transverse wavenumber) plane. A solution of the matrix equation then yields a solution for the Fourier transform of the currents $I_m^z(z)$ and $I_n^x(z)$. Each current function is then represented as an inverse Fourier transform, e.g., as

$$I_m^z(z) = \frac{1}{2\pi} \int_{C_i} \tilde{I}_m^z(k_z) e^{-jk_z z} dk_z \tag{6}$$

where path C_z runs from $-\infty$ to ∞ in the complex k_z (longitudinal wavenumber) plane.

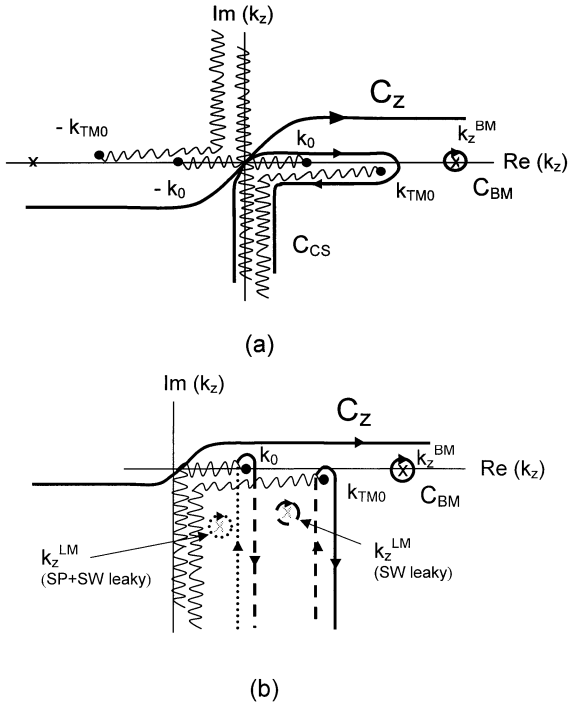

Fig. 2. Complex k_z-plane used to perform the inverse Fourier transform to construct the strip current. (a) The original path of integration C_z and its two constituent parts: an integration path $C_{\rm BM}$ around the BM pole on the real axis and an integration path $C_{\rm CS}$ around the branch cuts. (b) The integration path $C_{\rm CS}$ has been deformed to steepest descent paths that descend from the k_0 and $k_{\rm TM_0}$ branch points. LM poles that are captured during the path deformation are shown.

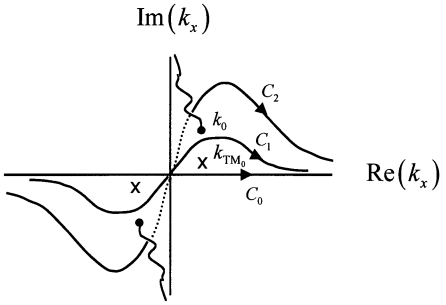

Fig. 3. Paths of integration in the k_x-plane that are used to find the various types of modes on the microstrip line. The path C_0 (real axis) is used to obtain the BMs of propagation. Path C_1 (deformed around the $\rm TM_0$ poles) is used to find the surface-wave LM solution. Path C_2 (around the $\rm TM_0$ poles and through the k_0 branch cuts) is used to obtain the space + surface-wave leaky solution.

The complex k_z-plane of integration is shown in Fig. 2(a). The path C_z is deformed around poles (path $C_{\rm BM}$) and branch points in the complex plane (path $C_{\rm CS}$). The poles on the real axis correspond to the BMs of the microstrip line. The branch points arise because of the multiple-value nature of the matrix terms in (5) [5] due to the fact that various paths of integration may be used when evaluating the integral in the k_x-plane that defines these terms [8]–[13]. For example, a path along the real axis may be used, or a path that is deformed around the poles of the spectral-domain Green's function in the k_x-plane, or a path that is also deformed around the branch points in the k_x-plane and lies partly on the lower (improper) sheet. As shown in [5], there are two types of branch points in the longitudinal wavenumber (k_z)-plane that the path C_z must be deformed around: one pair of branch points is at $\pm k_0$ and the others are at $\pm k_g$, where k_g is the wavenumber of a guided mode (sur-

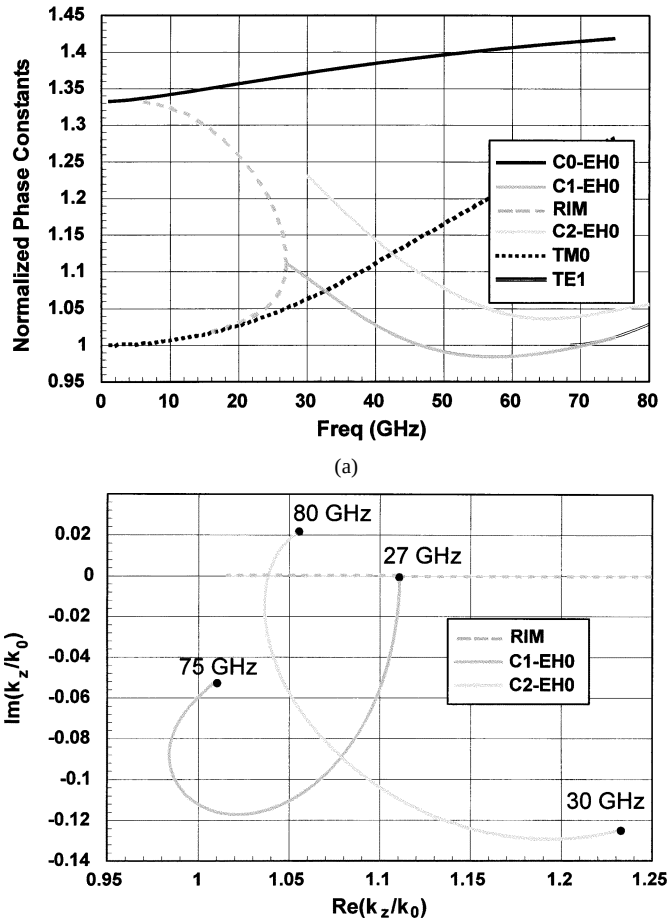

Fig. 4. (a) Plot of the normalized wavenumbers (β/k_0) for the modes of propagation on a microstrip line with $\varepsilon_r = 2.2$, $h = 1.0$ mm, and $w/h = 1$. The BM (C0-EH0), surface LM (C1-EH0), and space + surface-wave LM (C2-EH0) solutions are shown along with the dispersion curves of the $\rm TM_0$ and $\rm TE_1$ surface-wave modes of the grounded slab. (b) Plot of the real and imaginary parts of the normalized wavenumbers versus frequency showing the C1-EH0 and C2-EH0 modes.

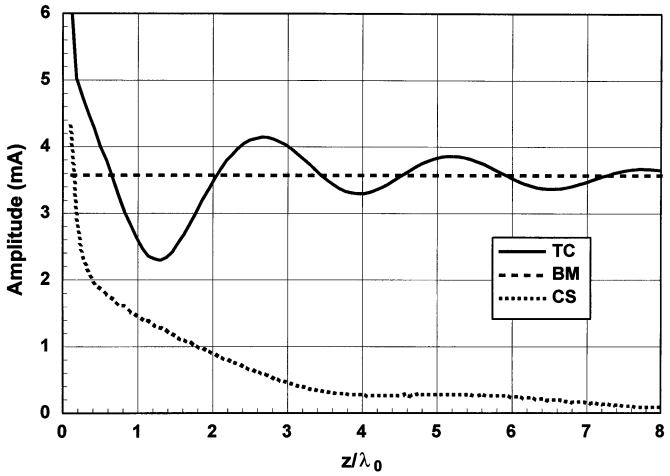

Fig. 5. Plot of the longitudinal current on the microstrip line versus distance from the source for the case of Fig. 4 at a frequency of 70 GHz. The TC is shown, along with its constituent parts, the BM and CS currents.

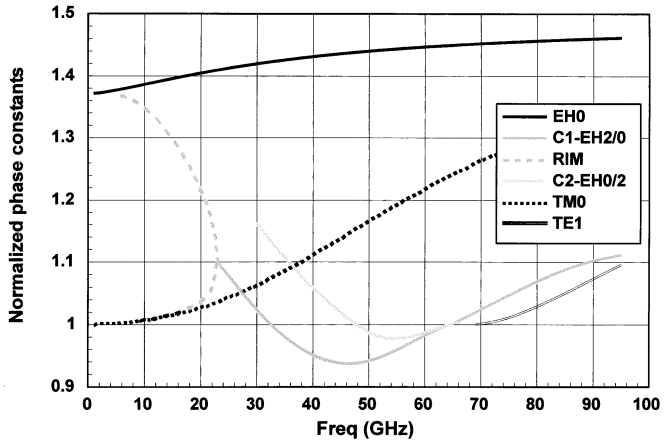

(a)

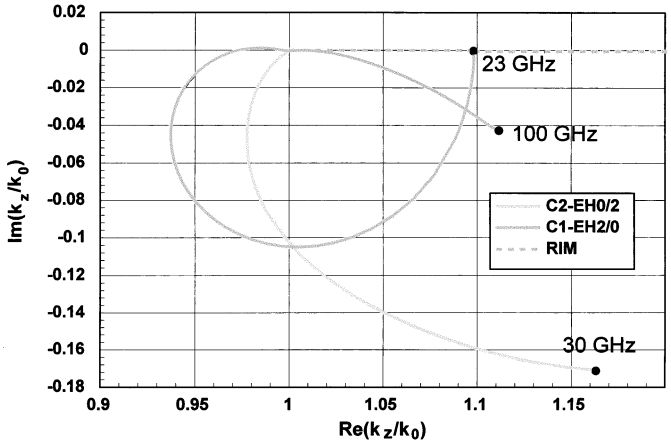

(b)

Fig. 6. (a) Plot of the normalized wavenumbers (β/k_0) for the modes of propagation on a microstrip line with $\varepsilon_r = 2.2$, $h = 1.0$ mm, and $w/h = 3$. The BM (C0-EH0), surface LM (C1-EH2/0), and space + surface-wave LM (C2-EH0/2) solutions are shown, along with the dispersion curves of the TM_0 and TE_1 surface-wave modes of the grounded slab. (b) Plot of the real and imaginary parts of the normalized wavenumbers versus frequency, showing the C1-EH2/0 and C2-EH0/2 modes.

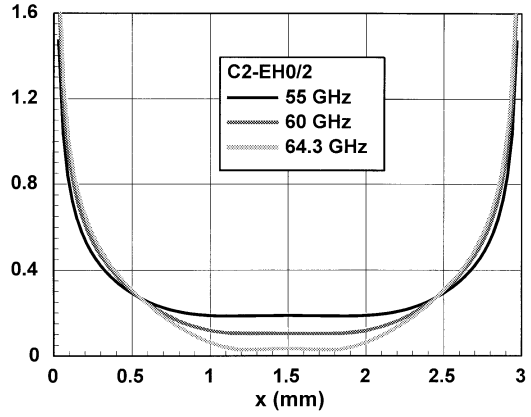

(a)

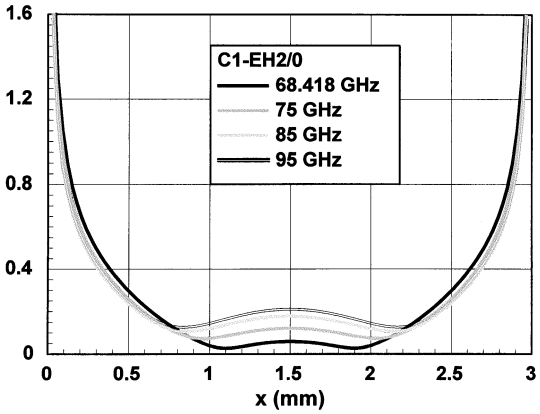

(b)

Fig. 7. Plot of the normalized longitudinal surface current density $J_{sz}(x)$ as a function of the transverse distance x across the strip for the case of Fig. 6. Results are shown for the C_2 solution (labeled C2-EH0/2) at three lower frequencies and the C_1 solution labeled (C1-EH2/0) at three higher frequencies.

face wave) of the grounded dielectric slab. Assuming that only the TM_0 mode of the slab is above cutoff, there will be only one pair of the second kind of branch points, as shown in Fig. 2(a). (As explained in [5], this pair of branch points appears on the sheet that the path of integration is on, but does not appear on the lower sheet of the k_0 branch point.) The original path of integration is equivalent to the path(s) C_{BM} around the BM pole(s) and the path C_{CS} around the branch points. The TC is then expressed as the sum of two parts: a part coming from the residue contributions from the BM poles and a part coming from the branch-cut integral. The first part defines the current of the BMs, while the second part defines the CS part of the current.

The path around the branch cuts may be further deformed to a set of two steepest descent paths that descend vertically from the branch points at k_0 and k_{TM_0}, as shown in Fig. 2(b). During this deformation, leaky-wave poles may be captured. A leaky-wave pole that lies in the region $k_0 < \beta_{\mathrm{LM}} < k_{\mathrm{TM}_0}$ will be captured if it lies on the lower sheet of the k_{TM_0} branch point corresponding to a LM on the microstrip line that leaks only into the TM_0 surface wave of the substrate. The path of integration in the k_x-plane for such a LM is the path C_1 shown in Fig. 3. A leaky-wave pole that lies in the region $\beta_{\mathrm{LM}} < k_0$ will be captured if it lies on the lower sheets of the k_0 and k_{TM_0} branch points. Such a LM leaks into both the TM_0 substrate mode and into space. The path of integration in the k_x-plane for this type of LM is the path C_2 shown in Fig. 3. If the LM pole is captured, the LM is said to be "physical." The CS current is, therefore, a sum of all physical LM currents plus two current waves that arise from the two steepest descent integrations shown in Fig. 2(b). These last two currents are called the "RW" currents and, in particular, they are labeled as the TM_0 and k_0 RW currents [3].

III. Results

In this investigation, a microstrip on a substrate with a relative permittivity of $\varepsilon_r = 2.2$ and a thickness of 1.0 mm is examined. Results are presented for various strip widths, corresponding to $w/h = 1, 3$, and 6. The first case is considered to be a moderate strip width, while the last two cases are wide strips.

A. Moderate Strip Width $(w/h = 1)$

A dispersion plot for $w/h = 1$ is shown in Fig. 4(a). The BM solution (C0-EH0) that is found from using the real-axis path of integration in the spectral-domain solution for the propagation on an infinite source-free line is shown along with the LM

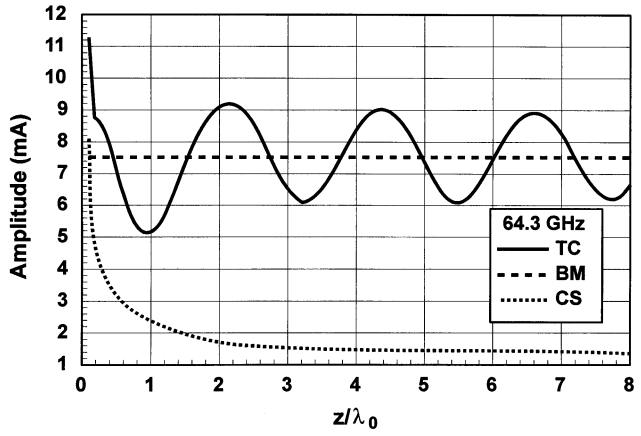

Fig. 8. Plot of the longitudinal current on the microstrip line versus distance from the source for the case of Fig. 6 at a frequency of 64.3 GHz. The TC is shown, along with its constituent parts, the BM and CS currents.

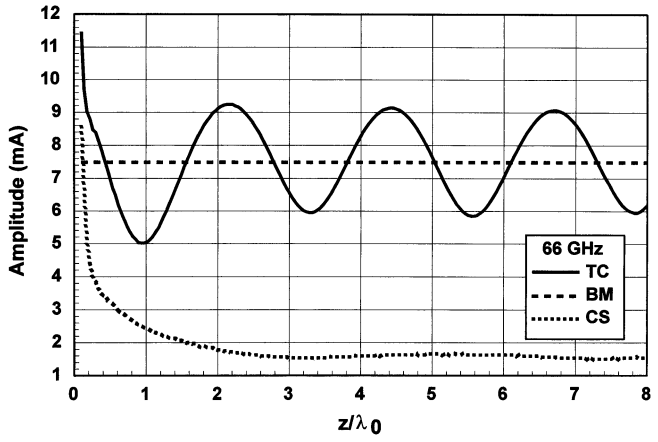

(a)

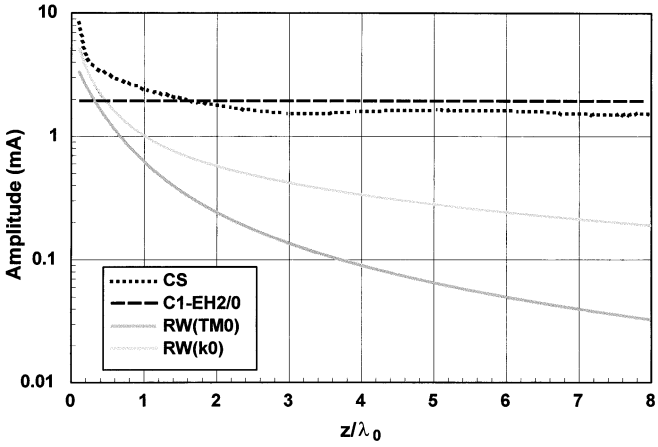

(b)

Fig. 9. Plot of the longitudinal current on the microstrip line versus distance from the source for the case of Fig. 6 at a frequency of 66 GHz. (a) The TC is shown, along with its constituent parts, the BM and CS currents. (b) The CS current is shown, along with its constituent parts, the C1-EH2/0 LM, k_0 RW, and TM_0 RW currents.

solutions that are found. The dispersion curve for the TM_0 and TE_1 surface-wave modes of the grounded slab are also shown. The BM solution is found from using the real-axis path of integration (C_0) and this mode has a current profile on the strip that is usually associated with a quasi-TEM (or EH_0) mode (a

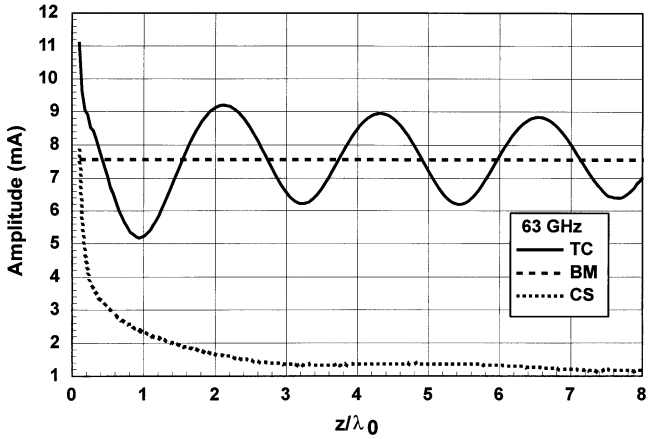

(a)

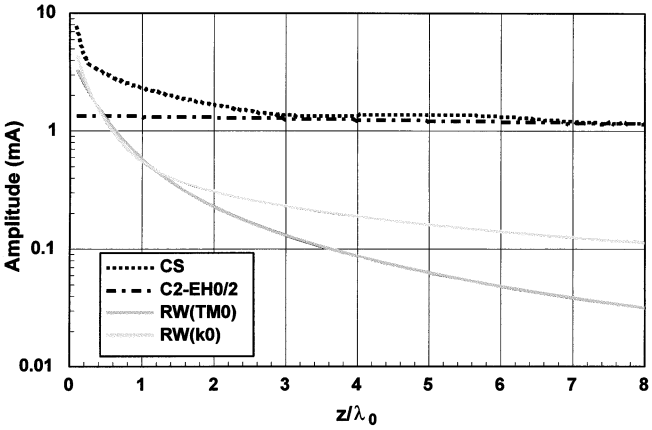

(b)

Fig. 10. Plot of the longitudinal current on the microstrip line versus distance from the source for the case of Fig. 6 at a frequency of 63 GHz. (a) The TC is shown, along with its constituent parts, the BM and CS currents. (b) The CS current is shown, along with its constituent parts, the C2-EH0/2 LM, k_0 RW, and TM_0 RW currents.

relatively uniform longitudinal current with edge singularities). Hence, the solution is designated as C0-EH0. A surface-wave LM (labeled C1-EH0) begins at approximately 26 GHz and becomes physical at 32 GHz, where it crosses the dispersion curve for the TM_0 surface-wave mode. (This mode is labeled C1-EH0 since the C_1 path in Fig. 3 is used in the spectral-domain solution for the propagation on an infinite source-free line to find this mode [1], [8]–[13] and the current profile is that of an EH_0 mode). It becomes nonphysical at 46 GHz, where it crosses the $\beta = k_0$ line. A space-wave leaky solution (labeled C2-EH0) is also found to exist, but this solution never becomes physical, as the phase constant is always above k_0. (The path C_2 in Fig. 3 is used in the spectral-domain analysis of the infinite line to obtain this solution.) Fig. 4(b) shows the trajectory of the two LM solutions in the k_z-plane, which simultaneously displays the phase and attenuation constants versus frequency. Although the phase constant of the surface LM crosses the $\beta = k_0$ line (twice), the attenuation constant remains high at these frequencies so that the trajectory does not approach near to the point $k_z = k_0$. Consequently, although the CS current increases in strength with frequency, the spurious oscillations die out relatively quickly with distance from the source. A typical result is shown in Fig. 5 at 70 GHz. The TC on the strip is plotted versus distance from the

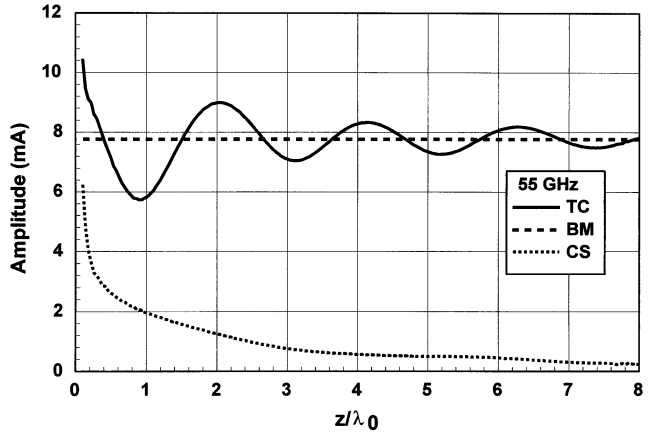

(a)

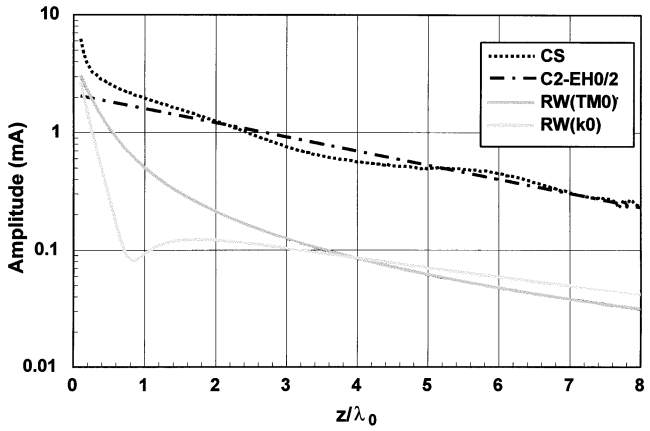

(b)

Fig. 11. Plot of the longitudinal current on the microstrip line versus distance from the source for the case of Fig. 6 at a frequency of 55 GHz. (a) The TC is shown, along with its constituent parts, the BM and CS currents. (b) The CS current is shown, along with its constituent parts, the C2-EH0/2 LM, k_0 RW, and TM_0 RW currents.

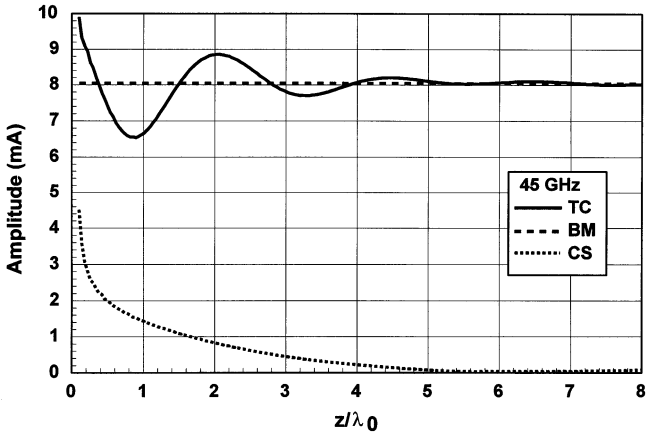

(a)

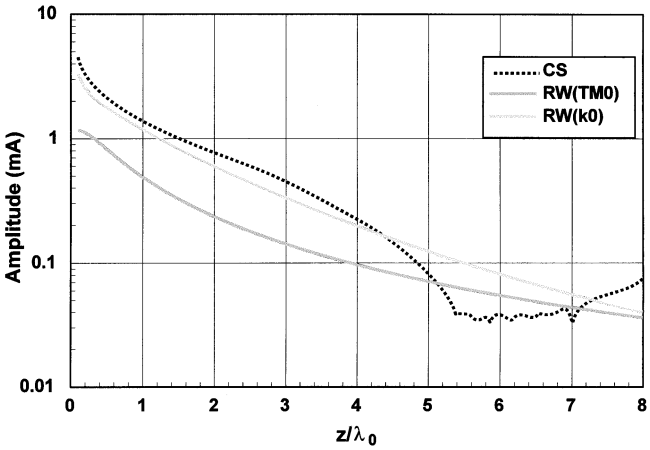

(b)

Fig. 12. Plot of the longitudinal current on the microstrip line versus distance from the source for the case of Fig. 6 at a frequency of 45 GHz. (a) The TC is shown, along with its constituent parts, the BM and CS currents. (b) The CS current is shown, along with its constituent parts, the k_0 RW, and TM_0 RW currents.

source, along with the two components of the TC, the BM current and the CS current. It is seen that the CS current decays fairly quickly with distance, which damps out the oscillations in the TC. Since there are no physical LMs at this frequency, there is no LM current, and the CS current is equal to the sum of the two RW currents. The RW currents cause a large spurious oscillation in the current due to the strong excitation of these currents at this high frequency, but the oscillations die out fairly quickly with distance from the source. This is in agreement with the conclusions reached in [3], where it was shown that, for moderate strip widths, the spurious oscillations in the TC caused by the CS current generally increase continuously with frequency, although LM effects are not very significant far away from the source.

B. Moderately Large Strip Width $(w/h = 3)$

A dispersion curve for the case $w/h = 3$ is shown in Fig. 6(a). The surface-wave leaky solution (labeled C1-EH2/0) begins at approximately 23 GHz (where it is nonphysical), and it becomes physical at approximately 27 GHz. It becomes nonphysical at approximately 32 GHz, and then becomes physical once again at approximately 64.3 GHz. The space + surface-wave leaky solution (labeled C2-EH0/2) becomes physical at approximately 48 GHz, and then becomes nonphysical at approximately 64.3 GHz. (The plot of this mode stops at 66.13 GHz, where the mode crosses the real axis in the k_z-plane and becomes a completely nonphysical "growing" mode with a negative attenuation constant.) Near 64.3 GHz, both the surface-wave leaky solution and space-wave leaky solution approach $\beta = k_0$. The trajectory plot in Fig. 6(b) shows that both of these LMs approach the point $k_z = k_0$ near this frequency. That is, the imaginary part of k_z (the negative of the attenuation constant) becomes very small when the real part of k_z (the phase constant) approaches k_0.

A plot of the transverse profile of the current, i.e., $J_{sz}(x)$, for the LMs on an infinite line are shown in Fig. 7 at various frequencies. (This is useful for explaining the mode designations and also for interpreting the nature of the modes that are responsible for the strong spurious oscillations that will be shown presently.) The C_2 LM has a current profile that resembles an EH_0 mode (quasi-uniform current with edge singularities) at low frequencies, but the current evolves into a profile that resembles more of an EH_2 shape at higher frequencies (hence, the designation EH0/2). The C_1 mode resembles an EH_2 mode at lower frequencies, but evolves more into an EH_0 type of mode at higher frequencies (hence, the designation C1-EH2/0).

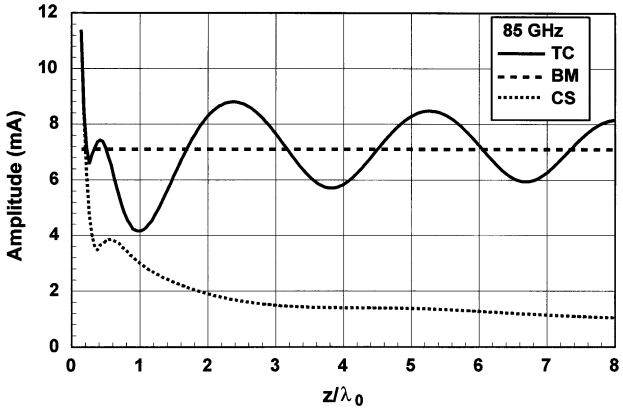

(a)

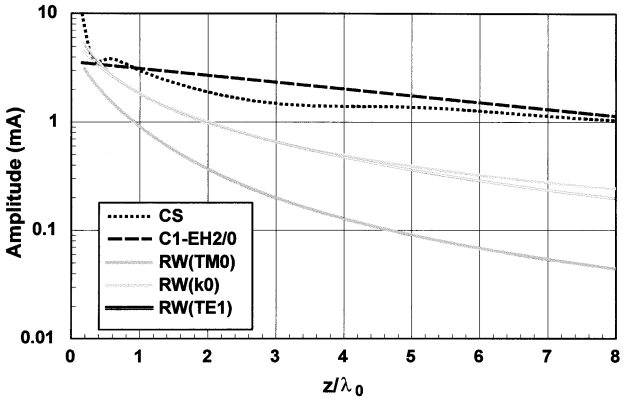

(b)

Fig. 13. Plot of the longitudinal current on the microstrip line versus distance from the source for the case of Fig. 6 at a frequency of 85 GHz. (a) The TC is shown, along with its constituent parts, the BM and CS currents. (b) The CS current is shown, along with its constituent parts, the C1-EH2/0 LM, k_0 RW, and TM_1 RW currents.

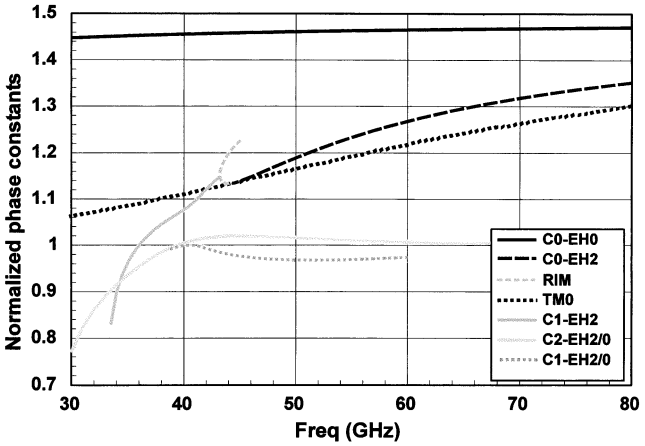

(a)

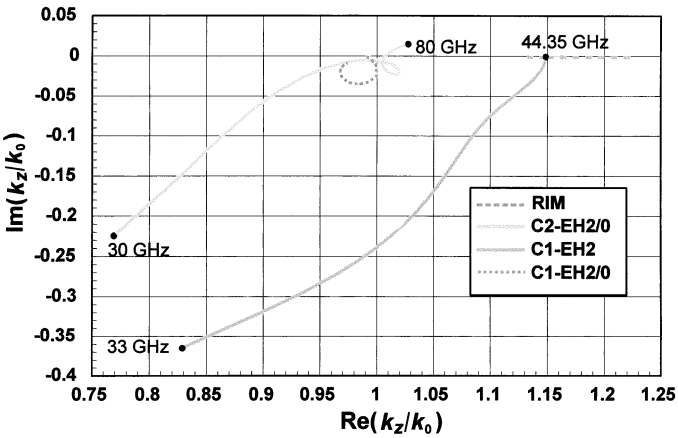

(b)

Fig. 14. (a) Plot of the normalized wavenumbers (β/k_0) for the modes of propagation on a microstrip line with $\varepsilon_r = 2.2$, $h = 1.0$ mm, and $w/h = 6$. The quasi-TEM BM (C0-EH0) solution is shown, along with a surface LM (C1-EH2/0) and a space + surface-wave LM (C2-EH0/2) solution. A higher order BM (C0-EH2) is also shown, which becomes a surface-wave LM solution (C1-EH2) below the cutoff frequency of 44.35 GHz. The dispersion curves of the TM_0 and TE_1 surface-wave modes of the grounded slab are also shown. (b) Plot of the real and imaginary parts of the normalized wavenumbers versus frequency, showing the C1-EH2, C1-EH2/0, and C2-EH2/0 modes.

A plot of the current on the microstrip line at 64.3 GHz is shown in Fig. 8. Note that the spurious oscillations in the TC show a *very small* decay with distance. In fact, at a distance of eight wavelengths, the oscillation amplitude is only slightly less than it was at a distance of one wavelength. This is because the CS current decays very slowly with distance, as shown in Fig. 8.

Fig. 9(a) shows the same type of result at a slightly higher frequency of 66 GHz, where the effect of a very slowly decaying CS current is still evident. At this frequency, only the C_1 LM solution is physical. In Fig. 9(b), the CS current has been resolved into its constituent parts, consisting of a physical C_1 LM and the two RW currents. Note that this LM accounts for almost all of the CS current, and that it has a nearly constant (flat) current versus distance z due to the small attenuation. Hence, it is a slowly attenuating C_1 LM that is responsible for the flat CS current at a frequency slightly above critical frequency of 64.3 GHz.

Fig. 10 shows results for a frequency of 63 GHz that is slightly below the critical frequency of 64.3 GHz. At this frequency, the C_1 LM has become nonphysical, thus, only the C_2 LM is a physical mode. Fig. 10(a) shows that the spurious oscillations persist to very large distances once again due to the flat CS current. Fig. 10(b) shows that the flat CS current is now due to a weakly attenuated C_2 mode. Hence, weakly attenuated LMs are found close to the critical frequency of 64.3 GHz on either side. Slightly below this frequency, the mode is a C_2 mode, with a current shape that is almost an equal split between EH_0 and EH_2 in field shape (see Fig. 7). Slightly above this frequency, the LM is a C_1 mode, with a current shape that is also a combination of EH_0 and EH_2 shapes (slightly more toward EH_2).

Fig. 11(a) shows the TC and its constituent parts at a lower frequency of 55 GHz. At this frequency, only the C2-EH0/2 LM solution is physical. Note that the oscillations in the TC die out much quicker with distance compared to the 63-GHz case of Fig. 10(a) since the CS current is not as flat with distance. Fig. 11(b) explains why this is the case. It is seen that the C2-EH0/2 LM attenuates much more rapidly with distance than for the LM at 63 GHz. The LM in Fig. 11(a) is found to have the profile of an EH_0 mode.

Fig. 12 presents results for a still lower frequency of 45 GHz. At this frequency, there are no physical LMs so the CS current consists of only the two RW currents [see Fig. 12(b)]. Fig. 12(a) shows that the TC decays rapidly with distance so that spurious

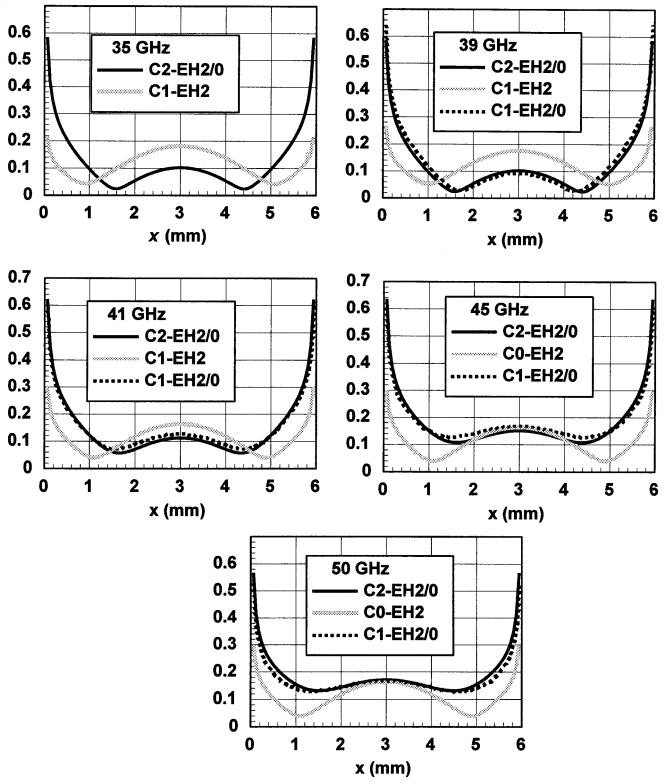

Fig. 15. Plot of the normalized longitudinal surface current density $J_{sz}(x)$ as a function of the transverse distance x across the strip for the case of Fig. 14. Results are shown for the C2-EH2/0, C1-EH2/0, and C1-EH2 solution (which becomes the C0-EH2 solution above the cutoff frequency of 44.35 GHz).

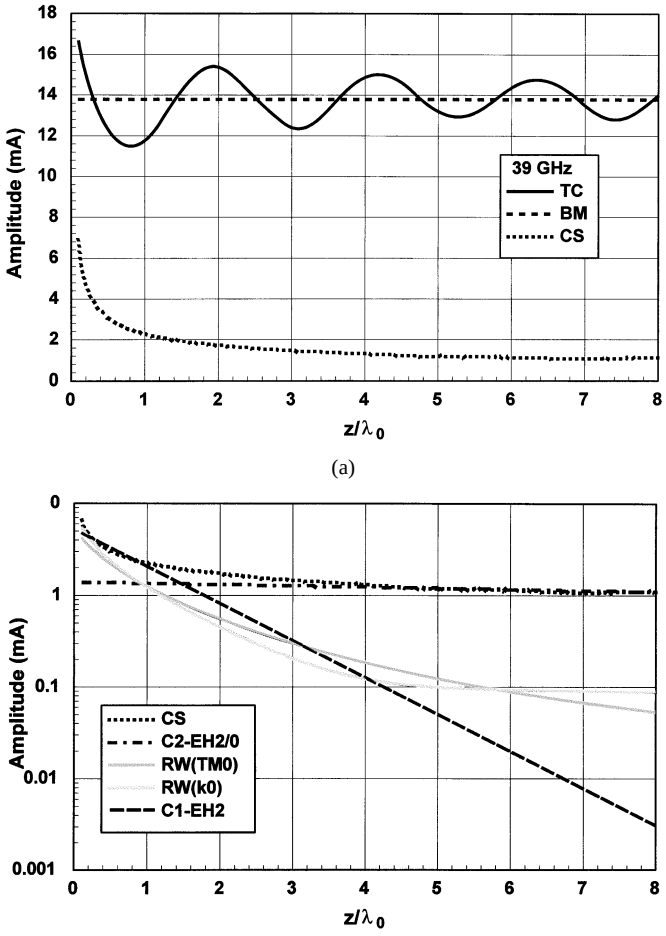

Fig. 16. (a) Plot of the longitudinal current on the microstrip line versus distance from the source for the case of Fig. 14 at a frequency of 39 GHz. (a) The TC is shown, along with its constituent parts, the BM and CS currents. (b) The CS current is shown, along with its constituent parts, the C2-EH2/0 LM, C1-EH2 LM, k_0 RW, and TM_0 RW currents.

effects are only important within a couple of wavelengths from the source. Furthermore, the overall level of the CS current is less than that for the 55 GHz case since there is no physical LM.

Fig. 13 shows results for 85 GHz, where the frequency is now significantly higher than the critical frequency of 64.3 GHz. At this frequency, the TE_1 surface wave of the slab is above cutoff (see Fig. 6). Hence, there are now three RW currents, the k_0 RW, TM_0 RW, and TE_1 RW, which, together with the LM current, compose the CS current. The C1-EH2/0 mode attenuates much more rapidly than for the case of Fig. 9 at 66 GHz. The CS current is likewise not as flat as that in Fig. 9, although the CS current in Fig. 13 is somewhat flatter than the LM current in Fig. 13, between about 3–8 wavelengths from the source. This is due to interference between the LM and RW currents.

C. Very Large Strip Width $(w/h = 6)$

The effect of long-range spurious oscillations is not limited to one particular strip width, but evidently occurs whenever the strip width is large. To demonstrate this, the case of a very wide strip $w/h = 6$ is considered. Fig. 14(a) shows the dispersion plot, while Fig. 14(b) shows the trajectory plot in the k_z-plane. The dispersion plot in Fig. 14(a) is more complicated than those for the previous two cases. In addition to the usual BM that has an EH_0 current profile, a higher order EH_2 BM exists above a cutoff frequency of 44.35 GHz. Below the cutoff frequency, the EH_2 mode first becomes an improper real mode and, finally, a LM below approximately 43 GHz. (The LM is one that leaks into the substrate mode and, hence, it is labeled as C1-EH2.) In addition to this mode, a pair of LMs is also found to exist. One is a space + surface-wave LM labeled C2-EH2/0. The other is a surface-wave LM labeled C1-EH2/0. (The plot for the C1-EH2/0 mode stops at 60 GHz since, at this frequency, the mode crosses the real axis in the k_z-plane to become a completely nonphysical "growing" mode with a negative attenuation constant.) These two LMs have an EH_2 profile at lower frequencies, but the profile changes to that of an EH_0 mode at higher frequencies (above approximately 40 GHz). These are the LMs that are responsible for the flat CS effect for this very wide strip. Both of these modes approach the branch point at k_0 near 39 GHz (a significantly lower frequency than the critical frequency of 64.3 GHz for the $w/h = 3$ case).

Fig. 15 shows a plot of the current profiles for these modes at various frequencies. It is seen that the C1-EH2 mode has the profile of an EH_2 mode, as expected, since this mode is the direct continuation of the EH_2 mode below cutoff. The C2-EH2/0 mode has an EH_2 shape below approximately 40 GHz, and above this frequency begins to look more like an EH_0 mode. The C1-EH2/0 mode has a current profile that closely matches that of the C2-EH2/0 mode at all frequencies, perhaps because of the fact that the dispersion plots are fairly close together. Note

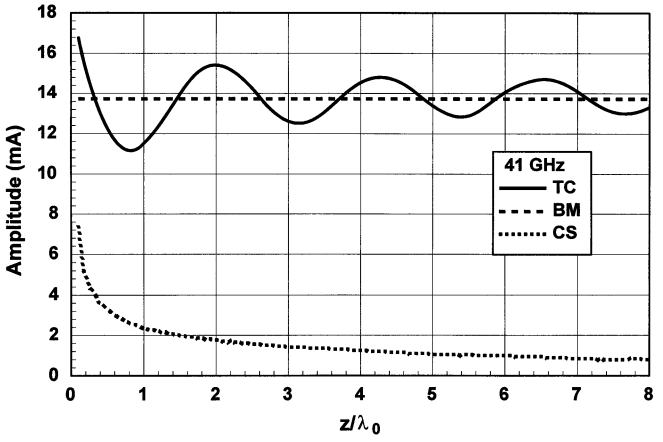

(a)

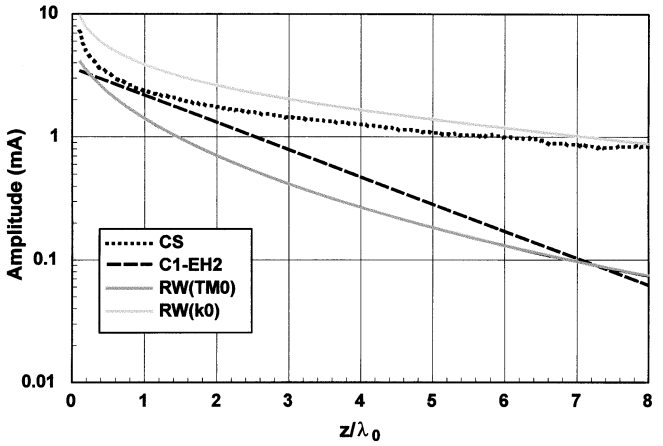

(b)

Fig. 17. (a) Plot of the longitudinal current on the microstrip line versus distance from the source for the case of Fig. 14 at a frequency of 41 GHz. (a) The TC is shown, along with its constituent parts, the BM and CS currents. (b) The CS current is shown, along with its constituent parts, the C1-EH2 LM, k_0 RW, and TM_0 RW currents.

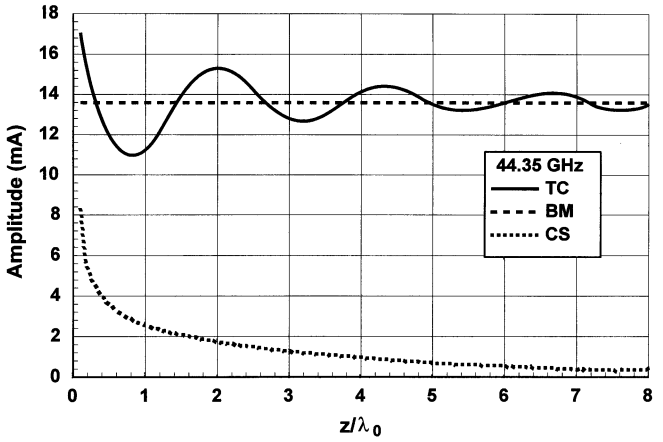

(a)

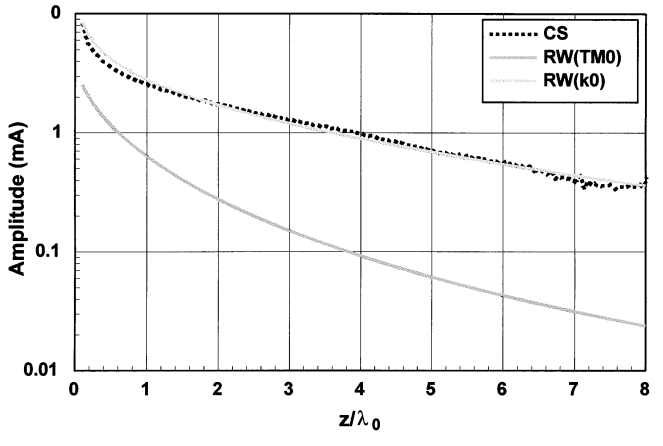

(b)

Fig. 18. (a) Plot of the longitudinal current on the microstrip line versus distance from the source for the case of Fig. 14 at a frequency of 44.35 GHz. (a) The TC is shown, along with its constituent parts, the BM and CS currents. (b) The CS current is shown, along with its constituent parts, the k_0 RW and TM_0 RW currents.

that the C2-EH2/0 mode is physical below 39 GHz, while the C1-EH2/0 mode never becomes physical.

A plot of the current at 39 GHz is shown in Fig. 16. The flat CS current in Fig. 16(a) results in spurious oscillations out to large distances, as for the previous case of $w/h = 3$ at 64.3 GHz. Fig. 16(b) shows that the weakly attenuated C2-EH2/0 mode is responsible for the flat CS current. The other LM that is physical is the C1-EH2 mode, but this mode decays much more rapidly with distance, and is not responsible for the flat CS current effect.

Fig. 17 shows results for a frequency of 41 GHz, which is slightly higher than the critical frequency of 39 GHz. At this frequency, the only physical LM is the C1-EH2 mode, but it attenuates rapidly with distance. The CS current is somewhat flat with distance, but this is now due to a fairly strong and slowly decaying k_0 RW current. The k_0 RW current is very strong because of the fact that the pole in the complex plane corresponding to the C2-EH2/0 mode is not captured (because the mode is nonphysical and is in the region $\beta > k_0$), but it is close to the k_0 steepest descent path at this frequency [the mode is close to the $\beta = k_0$ line in Fig. 14(a)]. Therefore, in accordance with the previous discussion of the CS, this pole does not appear as a discrete mode in the CS current, but it nevertheless has an important influence on the CS current due to its close proximity to the steepest descent path.

Fig. 18 shows results for a higher frequency of 44.35 GHz, which is the cutoff frequency of the EH_2 mode. At this frequency, there are no physical LMs. Fig. 18(a) shows that the oscillations in the TC die out fairly quickly with distance. The CS current is composed of the two RW currents (mainly the k_0 RW current) and it decays fairly quickly with distance, as seen in Fig. 18(b).

Fig. 19 shows results for a considerably higher frequency of 70 GHz. There are now two BMs (EH_0 and EH_2) and, hence, the BM current itself shows an oscillatory pattern from interference effects. The oscillations in the TC that are due to the CS current dampen out more quickly with distance than for the 39-GHz case. Nevertheless, the overall level of the oscillations is quite strong because of the fact that the k_0 RW current has become fairly strong at this high frequency, where the nonphysical pole is once again close to the steepest decent path.

Fig. 20 shows a lower frequency of 35 GHz, where only the C2-EH2/0 mode is physical. The oscillations in the TC die out fairly quickly with distance since the C2-EH2/0 mode has a fairly rapid attenuation at this frequency.

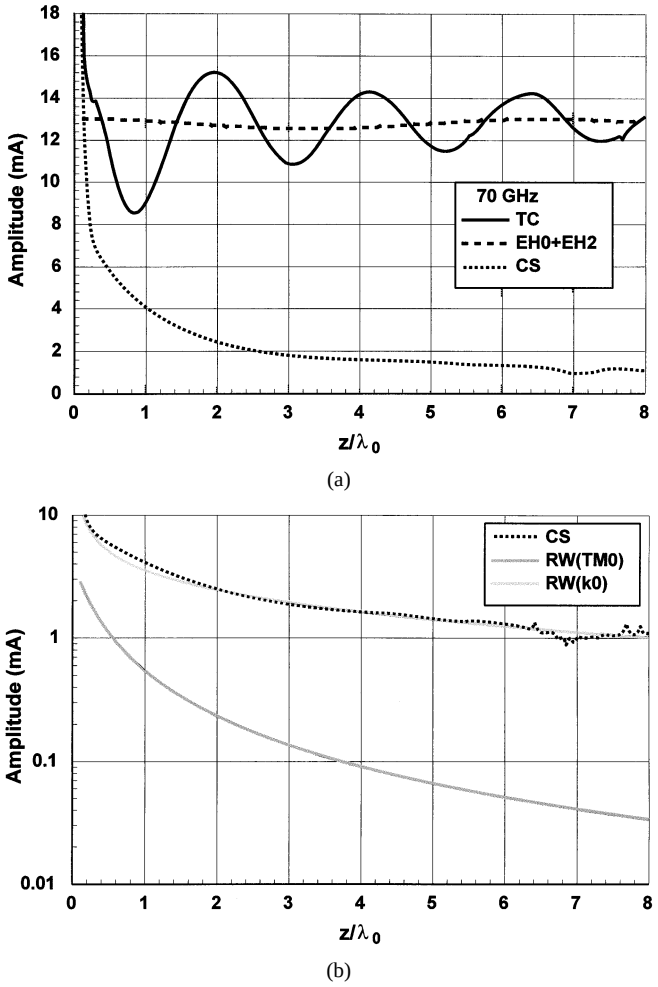

Fig. 19. (a) Plot of the longitudinal current on the microstrip line versus distance from the source for the case of Fig. 14 at a frequency of 70.0 GHz. (a) The TC is shown, along with its constituent parts, the BM and CS currents. (b) The CS current is shown, along with its constituent parts, the k_0 RW and TM_0 RW currents.

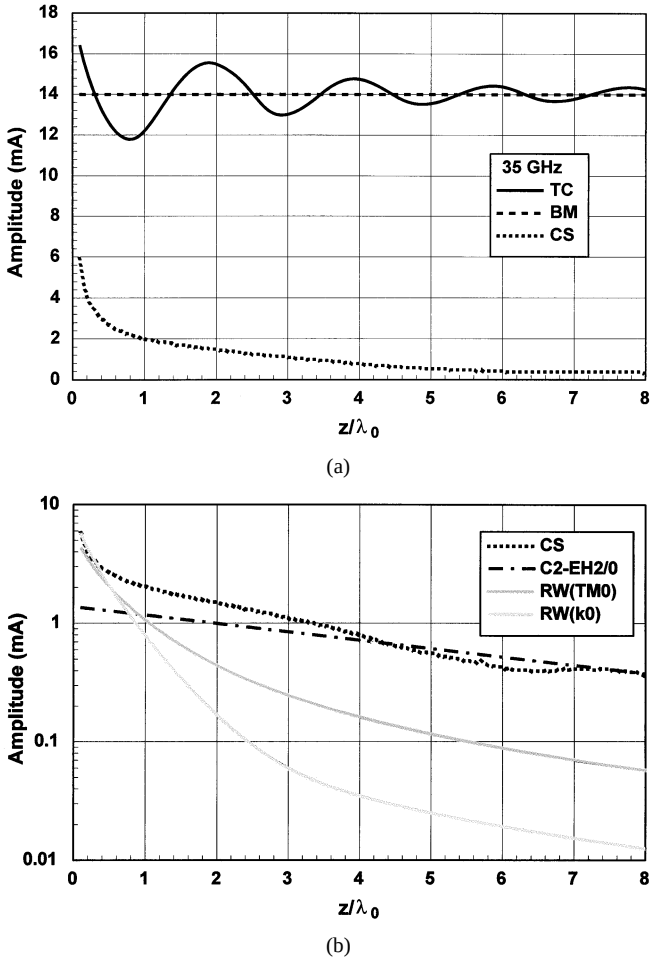

Fig. 20. (a) Plot of the longitudinal current on the microstrip line versus distance from the source for the case of Fig. 14 at a frequency of 35.0 GHz. (a) The TC is shown, along with its constituent parts, the BM and CS currents. (b) The CS current is shown, along with its constituent parts, the C2-EH2/0 LM, k_0 RW, and TM_0 RW currents.

D. Approximate Design Formula

It is found that an approximate equation for predicting the frequency where the spurious effects caused by the weakly attenuated LMs will occur, which is accurate for wide strips, is

$$f = \frac{c}{w\sqrt{\varepsilon_r - 1}} \tag{7}$$

with c being the speed of light in free space. This simple equation is relatively accurate for $w/h > 6$. For $w/h = 6$, this equation predicts 45.6 GHz, whereas the actual frequency for which maximum spurious effects occur is approximately 39 GHz. For $w/h = 3$, the formula predicts 91.2 GHz, whereas the actual frequency is approximately 64.3 GHz. Equation (7) is actually the formula for the cutoff frequency of the EH_2 mode, assuming perfect magnetic walls on the sides of the microstrip. It is noted from Fig. 14(a) that the cutoff frequency of the EH_2 mode is fairly close to the frequency at which the LMs approach the $\beta = k_0$ line, and this is the motivation for the empirical formula.

IV. Conclusions

Very severe spurious high-frequency effects may occur on microstrip line at certain frequencies when the strip width is large (approximately $w/h > 3$). These spurious effects are due to the excitation of weakly attenuated LMs on the line. The LMs are weakly attenuated because the corresponding poles in the complex longitudinal wavenumber (k_z)-plane approach the branch point $k_z = \pm k_0$ at a certain frequency, depending on the strip width.

For a microstrip line with a moderate strip width $(w/h < 3)$, the spurious effects observed in the current excited by a practical source increase with frequency and become important when the substrate thickness is about one-tenth of a free-space wavelength, as has been demonstrated previously. However, the spurious oscillations that are observed generally die out fairly quickly with distance from the source, and are largely confined to a region less than about ten wavelengths from the source. The spurious effects in this case are largely due to the RW currents that are excited by the source.

However, when the strip is wide, $(w/h > 3)$, the newly observed effect due to the excitation of weakly attenuated LMs

may result in significant spurious oscillations in the TC out to distances of many wavelengths from the source. The frequency at which this effect occurs decreases as the strip width increases. An approximate formula for predicting this frequency was given, which is relatively accurate when the strip width is very wide $(w/h > 6)$.

For moderately large strip widths $(w/h = 3)$, two types of LMs play a role in producing this spurious oscillation effect. A space + surface-wave LM is responsible for frequencies slightly less than the critical frequency (the frequency at which both modes approach the k_0 branch point), and a surface-wave leaky solution is responsible for frequencies slightly greater than the critical frequency. Both modes has a transverse current shape that is a combination of EH_0 and EH_2 shapes.

For very large strip widths $(w/h = 6)$, it is a space + surface-wave LM that is responsible for the spurious oscillation effect for frequencies slightly below the critical frequency. For frequencies slightly above the critical frequency the effect is due to a strong k_0 RW current, which is due to the presence of the space + surface-wave leaky pole in the complex plane, corresponding to the space + surface-wave LM that has now become nonphysical.

REFERENCES

[1] D. Nghiem, J. T. Williams, D. R. Jackson, and A. A. Oliner, "Existence of a leaky dominant mode on microstrip line with an isotropic substrate: Theory and measurements," *IEEE Trans. Microwave Theory Tech.*, vol. 44, pp. 1710–1715, Oct. 1996.

[2] M. Tsuji, H. Shigesawa, and A. A. Oliner, "Printed-circuit waveguide with anisotropic substrates: A new leakage effect," in *IEEE MTT-S Int. Microwave Symp. Dig.*, 1989, pp. 783–786.

[3] F. Mesa, D. R. Jackson, and M. Freire, "High frequency leaky-mode excitation on a microstrip line," *IEEE Trans. Microwave Theory Tech.*, vol. 49, pp. 2206–2215, Dec. 2001.

[4] C. DiNallo, F. Mesa, and D. R. Jackson, "Excitation of leaky modes on multilayer stripline structure," *IEEE Trans. Microwave Theory Tech.*, vol. 46, pp. 1062–1071, Aug. 1998.

[5] F. Mesa, C. Di Nallo, and D. R. Jackson, "The theory of surface-wave and space-wave leaky mode excitation on microstrip lines," *IEEE Trans. Microwave Theory Tech.*, vol. 47, pp. 207–215, Feb. 1999.

[6] D. R. Jackson, F. Mesa, M. Freire, D. P. Nyquist, and C. Di Nallo, "An excitation theory for bound modes, leaky modes, and residual-wave current on stripline structures," *Radio Sci.*, vol. 35, no. 2, pp. 495–510, Mar.-Apr. 2000.

[7] M. J. Freire, "Estudio del espectro modal delcampo electromagnetico excitado en lineas microtira," Ph.D. dissertation, Univ. Seville, Seville, Spain, 2000.

[8] J. Boukamp and R. H. Jansen, "Spectral domain investigation of surface wave excitation and radiation by microstrip lines and microstrip disk resonator," in *Proc. 13th Eur. Microwave Conf.*, Sept. 1983, pp. 721–726.

[9] K. A. Michalski and D. Zheng, "Rigorous analysis of open microstrip lines of arbitrary cross section in bound and leaky regimes," *IEEE Trans. Microwave Theory Tech.*, vol. 37, pp. 2005–2010, Dec. 1989.

[10] N. K. Das and D. M. Pozar, "Full-wave spectral-domain computation of material, radiation, and guided wave losses in infinite multilayered printed transmission lines," *IEEE Trans. Microwave Theory Tech.*, vol. 39, pp. 54–63, Jan. 1991.

[11] J. M. Grimm and P. P. Nyquist, "Spectral analysis considerations relevant to radiation and leaky modes of open-boundary microstrip transmission line," *IEEE Trans. Microwave Theory Tech.*, vol. 41, pp. 150–153, Jan. 1993.

[12] D. Nghiem, J. T. Williams, D. R. Jackson, and A. A. Oliner, "Proper and improper dominant mode solutions for stripline with an air gap," *Radio Sci.*, vol. 28, no. 6, pp. 1163–1180, Nov.–Dec. 1993.

[13] D. P. Nyquist and D. J. Infante, "Discrete higher-order leaky-wave modes and the continuous spectrum of stripline," *IEICE Trans.*, vol. E78-C, pp. 1331–1338, Oct. 1995.

[14] H. Shigesawa, M. Tsuji, and A. A. Oliner, "Conductor-backed slot line and coplanar waveguide: Dangers and full-wave analysis," in *IEEE MTT-S Int. Microwave Symp. Dig.*, 1988, pp. 199–202.

[15] ——, "Dominant mode power leakage from printed-circuit waveguide," *Radio Sci.*, vol. 26, pp. 559–564, Mar.–Apr. 1991.

[16] J.-Y. Ke, I.-S. Tsai, and C. H. Chen, "Dispersion and leakage characteristics of coplanar waveguides," *IEEE Trans. Microwave Theory Tech.*, vol. 40, pp. 1970–1973, Oct. 1992.

[17] H. Shigesawa, M. Tsuji, and A. A. Oliner, "The nature of the spectral-gap between bound and leaky solution when dielectric loss is present in printed-circuit lines," *Radio Sci.*, vol. 28, no. 6, pp. 1235–1243, Nov.–Dec. 1993.

[18] J. L. Cina and L. Carin, "Mode conversion and leaky-wave excitation at open-end coupled-microstrip discontinuities," *IEEE Trans. Microwave Theory Tech.*, vol. 43, pp. 2066–2071, Sept. 1995.

[19] H. Shigesawa, M. Tsuji, and A. A. Oliner, "A simultaneous propagation of bound and leaky dominant modes on printed-circuit lines: A new general effect," *IEEE Trans. Microwave Theory Tech.*, vol. 43, pp. 3007–3019, Dec. 1995.

[20] G.-J. Chou and C.-K. C. Tzuang, "Oscillator-type active-integrated antenna: The leaky mode approach," *IEEE Trans. Microwave Theory Tech.*, vol. 44, pp. 2265–2272, Dec. 1996.

[21] Y.-D. Lin and J.-W. Sheen, "Mode distinction and radiation-efficiency analysis of planar leaky-wave line source," *IEEE Trans. Microwave Theory Tech.*, vol. 45, pp. 1672–1680, Oct. 1997.

[22] G. W. Hanson and A. D. Yakolev, "An analysis of the leaky-wave dispersion phenomena in the vicinity of cutoff using complex frequency plane singularities," *Radio Sci.*, vol. 33, no. 6, pp. 803–819, July–Aug. 1998.

[23] J. Zehentner and J. Machac, "Properties of CPW in the sub-mm wave range and its potential to radiate," in *IEEE MTT-S Int. Microwave Symp. Dig.*, 2000, pp. 1061–1064.

[24] F. Mesa, A. A. Oliner, D. R. Jackson, and M. J. Freire, "The influence of a top cover on the leakage from microstrip line," *IEEE Trans. Microwave Theory Tech.*, vol. 48, pp. 2240–2248, Dec. 2000.

[25] W. L. Langston, J. T. Williams, D. R. Jackson, and F. Mesa, "Spurious radiation from a practical source on a covered microstrip line," *IEEE Trans. Microwave Theory Tech.*, vol. 49, pp. 2216–2226, Dec. 2001.

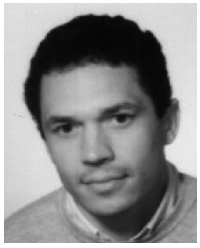

Francisco Mesa (M'94) was born in Cádiz, Spain, in April 1965. He received the Licenciado and Doctor degrees from the University of Seville, Seville, Spain, in 1989 and 1991, respectively, both in physics.

He is currently an Associate Professor in the Department of Applied Physics I, University of Seville. His research interest focuses on electromagnetic propagation/radiation in planar lines with general anisotropic materials.

David R. Jackson (S'83–M'84–SM'95–F'99) was born in St. Louis, MO, on March 28, 1957. He received the B.S.E.E. and M.S.E.E. degrees from the University of Missouri, Columbia, in 1979 and 1981, respectively, and the Ph.D. degree in electrical engineering from the University of California at Los Angeles (UCLA), in 1985.

From 1985 to 1991, he was an Assistant Professor in the Department of Electrical and Computer Engineering, University of Houston, Houston, TX. From 1991 to 1998, he was an Associate Professor in the same department and, since 1998, he has been a Professor. His current research interests include microstrip antennas and circuits, LW antennas, leakage and radiation effects in microwave integrated circuits, periodic structures, electromagnetic compatibility (EMC), and bioelectromagnetics. He is an Associate Editor for the *International Journal of RF and Microwave Computer-Aided Engineering*. He was an Associate Editor for *Radio Science*.

Dr. Jackson is the chapter activities coordinator for the IEEE Antennas and Propagation Society (IEEE AP-S) and the chair of the Technical Activities Committee for URSI, U.S. Commission B. He is also a distinguished lecturer for the IEEE AP-S Society. He was an associate editor for the IEEE TRANSACTIONS ON ANTENNAS AND PROPAGATION. He is a past member of the IEEE AP-S Administrative Committee (AdCom).